Review

Overview on the applications of random wave concept in coastal engineering

By Yoshimi GODA[*1,*2,†]

(Communicated by Kiyoshi HORIKAWA, M.J.A.)

Abstract: When "coastal engineering" was recognized as a new discipline in 1950, the significant wave concept was the basic tool in dealing with wave actions on beach and structures. Description of sea waves as the random process with spectral and statistical analysis was gradually introduced in various engineering problems in coastal engineering through the 1970s and 1980s. Nowadays the random wave concept plays the central role in engineering manuals for maritime structure designs. The present paper overviews the historical development of random wave concept and its applications in coastal engineering.

Keywords: coastal engineering, random waves, wave spectrum, wave statistics, sea waves, engineering applications

Introduction — Start of coastal engineering

Since old times, people have been aware of morphological changes of coastal areas and tried to protect the land from coastal erosion. They built coastal dikes, seawalls, jetties, and other structures. People made use of natural harbors for fishing, commerce and daily living. Where coastal topography provides no adequate harbors, people developed artificial harbors by constructing breakwaters and quays. The Allied Force's landing operation at Normandy Coast in June 1944 was a special example of artificial harbor construction in a very short time.

The Second World War also produced an innovation in wave forecasting method. Before 1942, harbor engineers employed some empirical formulas to correlate the height of sea waves with the wind speed and the fetch length (sea distance over which winds blow). Engineers and mariners described the magnitude of sea waves with a single height and single period through their visual judgment. No reliable wave recorders were available in the early 20th century.

Under an urgent request of the US Armed Forces, Sverdrup and Munk[1),2)] succeeded in developing a scientific method of wave forecasting with the new concept of significant wave, which was widely applied in many amphibious operations during World War II. Through laboratory measurements of waves generated by winds, Sverdrup and Munk were fully aware of wave randomness, but they needed a simple definition of wave height and period to correlate observed wave data with wind characteristics. They took the arithmetic means of the heights and periods of the highest one-third waves among a record of many waves, and called the wave having the averaged height and period of the highest one-third waves as the significant wave: the notations of $H_{1/3}$ and $T_{1/3}$ have been used since then. Wave forecasting was made in terms of the significant wave, and the propagation and transformation of the significant wave were analyzed with the then-available knowledge on the behavior of regular waves.

The new development on wave science and technology during World War II together with coastal protection methodology, ocean oil exploitation development, and other new knowledge were displayed to the audience at a specialty conference

*1 Professor Emeritus at Yokohama National University, Kanagawa, Japan.
*2 ECOH Corporation, Tokyo, Japan.
† Correspondence should be addressed: Y. Goda, ECOH Corporation, 2-6-4 Kita-Ueno, Taito-Ku, Tokyo 110-0014, Japan (e-mail: goda@ecoh.co.jp).

doi: 10.2183/pjab/84.374

at Long Beach, California in 1950. It attracted attentions of many specialists from different disciplines such as civil engineers, physical oceanographers, geologists, meteorologists, and others, and a new discipline of "coastal engineering" was established. Since then, various conferences on coastal engineering have periodically been held in Japan and other countries as well as internationally.

Spectral approach to random sea waves

Like any other physical process dealing with spectral concept, sea waves have been analyzed in the form of spectral functions. In the late 1940s and the early 1950s, waves were mostly recorded with the pressure gauges mounted on the seabed. The amplitudes of individual oscillations of the pressure records were converted to the amplitudes of surface waves with the pressure transfer function derived from the classical wave theory. Roll papers of pressure records were also photo-electronically treated to yield primitive data of frequency wave spectra.[3] In the 1950s and afterwards, improvements have been made in the wave recorders and the equipment for spectral analysis, and the database of frequency wave spectra was gradually expanded.

Another approach to the frequency wave spectrum was to visually measure the heights and periods of individual waves and to construct the joint frequency table of class-wise wave height and period. Based on this approach, Neumann[4] proposed the following functional form of wave spectrum with the exponents of $m = 6$ and $n = 2$ in 1953:

$$S(f) = Af^{-m} \exp[-Bf^{-n}] \tag{1}$$

where A and B are the constants and f is the frequency. Neumann's spectrum was utilized in the spectral wave forecasting method by Pierson, Neumann and James,[5] which also introduced the concept of directional spectrum or the directional spreading of wave energy.

Bretschneider[6] also proposed the wave spectrum of Eq. [1] with the exponents of $m = 5$ and $n = 4$ in 1959, based on the wave records obtained with the step-resistance wave gauges. He expressed the coefficients A and B in terms of the significant wave height $H_{1/3}$ and period $T_{1/3}$, but the expressions were later modified by Mitsuyasu[7] to be compatible with the statistical theory of sea waves.

On the basis of various instrumentally analyzed spectral data, Pierson and Moskowitz[8] in 1964 proposed the wave spectrum of Eq. [1] with the constant A as a function of wind speed and the exponents of $m = 5$ and $n = 4$. The spectrum is for fully developed wind waves. For the spectrum of developing seas, Hasselmann *et al.*[9] have proposed the so-called JONSWAP spectrum, which has the wind speed as the input parameter. When expressed in terms of the representative wave height and period, it has the following functional form:[10]

$$S(f) = \beta_J H_{1/3}^2 T_p^{-4} f^{-5} \times \exp[-1.25(T_p f)^{-4}]\gamma^{\exp[-(T_p f-1)^2/2\sigma^2]} \tag{2}$$

where β_J is a dimensionless constant being a function of γ, T_p denotes the period corresponding to the spectral peak frequency, γ is called the peak enhancement factor being given the value of 1 to 7 depending the state of wave development, and σ is a constant having the value of 0.07 for $f \le f_p$ and 0.09 for $f > f_p$. For the case of $\gamma = 1$ that corresponds to fully developed wind waves, the frequency spectrum is expressed as the functions of the significant wave height $H_{1/3}$ and period $T_{1/3}$ as follows:[10]

$$S(f) = 0.205 H_{1/3}^2 T_{1/3}^{-4} f^{-5} \exp[-0.75(T_{1/3} f)^{-4}] \tag{3}$$

Equations [2] and [3] are utilized when constructing the frequency spectrum from the input data of wave height $H_{1/3}$ and period $T_{1/3}$.

The energy of sea waves spreads not only in the frequency band but also in the range of azimuth. Thus, the wave spectrum is normally expressed as the product of the frequency spectrum $S(f)$ and the directional spreading function $G(f;\theta)$ as follows:

$$S(f,\theta) = S(f)G(f;\theta) \tag{4}$$

The function $S(f,\theta)$ is called the directional wave spectral density function or the directional wave spectrum. It has the dimension of $m^2 \cdot s/rad$ or the equivalent units. The frequency spectrum $S(f)$ has the dimension of $m^2 \cdot s$, while the directional spreading function $G(f;\theta)$ has no dimension under the normalization condition such that the integral over the full azimuth range should be unity.

A number of field measurements have been carried out for clarification of the functional form of $G(f;\theta)$. Currently, the following function by Mitsuyasu *et al.*[11] is used as a standard form for engineering applications:

$$G(f;\theta) = G_0 \cos^{2s}\left(\frac{\theta-\theta_0}{2}\right) \quad [5]$$

where G_0 is a constant to satisfy the normalization condition, s represents the spread parameter, and θ_0 denotes the principal wave direction. A unique feature of the Mitsuyasu-type spreading function is the frequency dependency of the spread parameter as below.

$$s = \begin{cases} s_{\max} \cdot (f/f_p)^5 & : \quad f \le f_p \\ s_{\max} \cdot (f/f_p)^{-2.5} & : \quad f > f_p \end{cases} \quad [6]$$

Mitsuyasu *et al.*[11] have formulated the maximum value of spreading parameter $s_{\max}$ as a function of the state of wind-wave growth. When Goda and Suzuki[12] introduced Eqs. [5] and [6] for engineering applications in 1975, they proposed the values of $s_{\max} = 10$, 25 and 75 for wind waves, swell with short decay distance, and swell with long decay distance, respectively, together with a diagram of the increase of $s_{\max}$ in shallow water owing to wave refraction effect. The proposed $s_{\max}$ values are still employed in many case studies.

Figure 1 illustrates the crest pattern of wind waves, which was created by numerical simulation using the frequency spectrum of Eq. [3] and the directional spreading function of Eqs. [5] and [6] with $s_{\max} = 10$. The abscissa and ordinate are the Cartesian coordinates normalized with the deep-water wavelength $(L_p)_0$ corresponding to the spectral peak frequency. The shaded area indicates the surface elevation being higher than $0.1\eta_{\mathrm{rms}}$, where η_{rms} denotes the root-mean-square value of surface fluctuation under wave motion.

In 2001, Ewans[13] reported the result of the analysis of a directional wave buoy data of swell recorded off the west coast of the North Island of New Zealand. The swell that had traveled over the Southern Indian Ocean yielded the directional spreading equivalent to $s_{\max} = 65$. This result provides a supporting evidence for the assignment of $s_{\max} = 75$ for the swell with long decay distance proposed by Goda and Suzuki.[12]

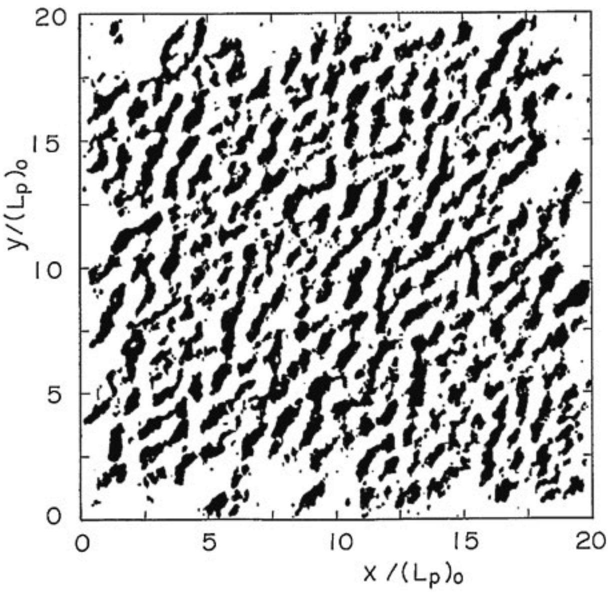

Fig. 1. Crest pattern of wind waves with $s_{\max} = 10$ created through numerical simulation.

Statistical properties of radom wave heights and periods

Directional spectral analysis of sea waves can reveal only one part of their characteristics. As we experience while standing in beach water, individual waves exert large forces on our body. Maritime structures such as breakwaters, seawalls, piers, and others must withstand strong actions of waves. The heights and periods of individual waves become important in the analysis of waves and their actions. Figure 2 exhibits an excerpt of an actual surface wave profile recorded in the field.

It is customary in coastal engineering to define individual waves at the points where the surface profile crosses the zero line (mean water level) upward or downward. The upward zero-crossing method is employed in Fig. 2, where small open circles indicate the zero-upcrossing points. The wave height is defined as the vertical distance between the highest and lowest elevations during the successive two zero-upcrossing points. The wave period is the time difference between the successive two zero-upcrossing points. In the example of Fig. 2, twenty one waves are defined by this method, but field wave measurements are usually conducted for the duration of twenty minutes from which around one hundred waves are defined and analyzed.

Although a record of individual waves gives impression of randomness, the distribution of individual wave heights approximately follows the Rayleigh distribution of the following:

$$p(x)dx = \frac{\pi}{2} x \exp\left[-\frac{\pi}{4}x^2\right]dx \quad : \quad x = H/\bar{H} \quad [7]$$

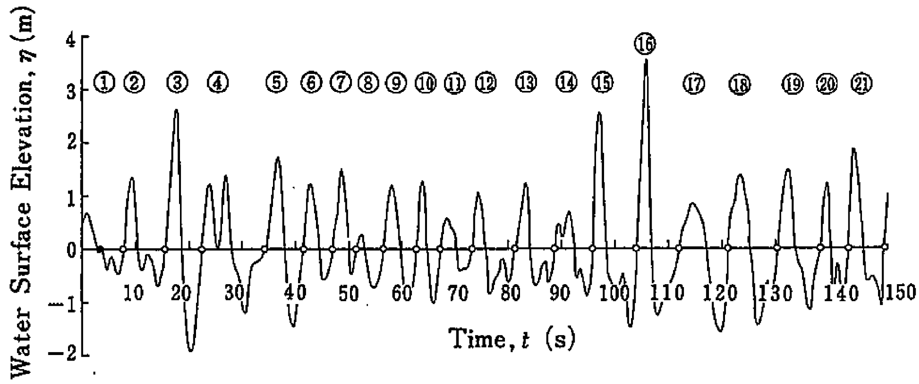

Fig. 2. Excerpt of a surface wave profile recorded in the field.

where $p(x)$ denotes the probability density function and $\bar{H}$ is the mean wave height. Longuet-Higgins[14)] applied the theory of Rayleigh distribution for sea waves under the assumption that the wave spectrum is narrow banded. He derived the theoretical relationships between several representative wave heights such as $\bar{H}$, $H_{1/3}$, $H_{\max}$ and others.

According to the Rayleigh distribution, the significant wave height $H_{1/3}$ is equal to $4.0\eta_{\rm rms} = 4.0\sqrt{m_0}$, where m_0 denotes the zero-th moment of frequency spectrum. Actual wave records show the wave height distribution slightly narrower than the Rayleigh with the average relation of $H_{1/3} \cong 3.8\eta_{\rm rms}$. A number of studies have been made since Longuet-Higgins to examine the wave height distribution for broad-band spectra. A recent study by Goda and Kudaka[15)] demonstrated that the distribution is controlled by the spectral shape parameter $\kappa(T_{01})$ defined as:

$$\kappa(T_{01})^2 = \left|\frac{1}{m_0}\int_0^\infty S(f)\cos 2\pi f T_{01} df\right|^2 + \left|\frac{1}{m_0}\int_0^\infty S(f)\sin 2\pi f T_{01} df\right|^2 \qquad [8]$$

where T_{01} is the mean period defined by the zero-th and first spectral moment as $T_{01} = m_0/m_1$.

As the spectral peak becomes sharp, the parameter κ takes a value near to 1, and it approaches 0 as the spectrum becomes flat. The effect of the spectral shape parameter on wave height parameters is exhibited in Fig. 3, where the ordinate is the ratio of the zero-crossing significant wave height $H_{1/3}$ to the root-mean-square wave amplitude $\eta_{\rm rms}$. The symbols with horizontal and vertical lines are the field data from various

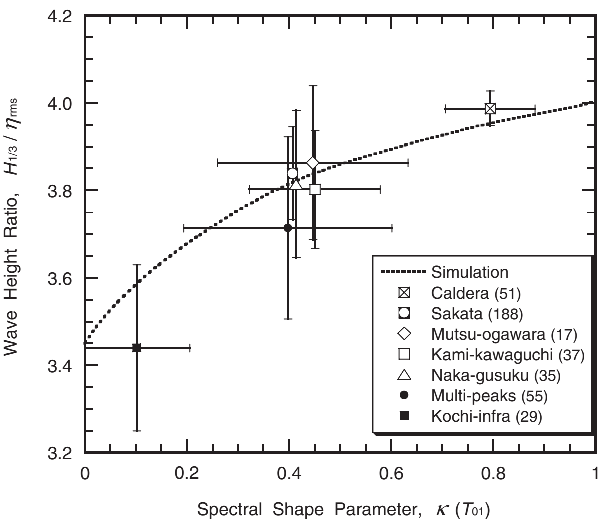

Fig. 3. Wave height ratio $H_{1/3}/\eta_{\rm rms}$ versus spectral shape parameter κ (T_{01}) for field measurement data after Goda and Kudaka.[15)]

locations listed in the legends with the numbers of wave records within the parentheses. The symbols are located at their mean values, while the lengths of the horizontal and vertical lines are set to equal to twice the standard deviations. The dashed line in Fig. 3 represents the approximate relationship between $H_{1/3}/\eta_{\rm rms}$ and $\kappa(T_{01})$, which has been obtained through analysis of wave simulation results. With the increase of κ toward 1 (spectrum become narrow-banded), the ratio $H_{1/3}/\eta_{\rm rms}$ approaches the theoretical value of 4.0. Though the field data exhibit large scatters owing to the statistical variability inherent to small sample sizes (around 100 waves) of ordinary wave records, the field data follow the empirical relationship derived through numerical simulation studies.

While the individual wave heights show the distribution close to the Rayleigh regardless of spectral shapes, the distribution of individual wave periods is strongly affected by the functional shape of wave frequency spectrum. For single peaked spectra, however, the following mean relationship has been observed:

$$T_{\max} \cong T_{1/10} \cong T_{1/3} \cong 1.2\bar{T} \qquad [9]$$

where $T_{\max}$ and $T_{1/10}$ are the period of highest wave and the average period of highest one-tenth waves.

The effects of wave spectral shape on the representative wave heights and periods as well as on their statistical variability have been investigated by Goda[10] and listed in his book.[16] Statistical variability is the inherent characteristic of random waves, because wave records are taken for a limited length of time only and they are subject to sample variability.

Analysis of wave transformations by means of wave spectrum

The first effort to evaluate the transformation of directional random waves was made by Pierson *et al.*[17] in 1952 for wave refraction in the northern New Jersey coast. The effort was overlooked by coastal engineers at that time, because they just began to use the concept of significant wave as equal to regular waves. A breakthrough was made by Karlsson[18] in 1969, who used the energy balance equation of directional wave spectral density for solving wave transformation of shoaling and refraction when waves propagate from deep water toward the shore. The equation is expressed as follows:

$$\frac{\partial}{\partial x}(Sv_x) + \frac{\partial}{\partial y}(Sv_y) + \frac{\partial}{\partial \theta}(Sv_\theta) = 0 \qquad [10]$$

where θ is the wave direction and v_x, v_y, and v_θ are given by

$$\left.\begin{aligned} v_x &= c_G \cos\theta, \\ v_y &= c_G \sin\theta, \\ v_\theta &= \frac{c_G}{c}\left(\frac{\partial c}{\partial x}\sin\theta - \frac{\partial c}{\partial y}\cos\theta\right) \end{aligned}\right\} \qquad [11]$$

The symbols c and c_G denote the phase and group velocities, respectively.

While Karlsson's work did not attract attention of coastal engineers in US and Europe, Nagai *et al.*[19] employed this model to compute wave transformation for actual harbor designs. Goda and Suzuki[12] also used Karlsson's model to compute the refraction coefficient of random waves defined with the Mitsuyasu-type directional spreading function. They also demonstrated a large difference between monochromatic (regular) waves and multidirectional random waves with respect to the wave height variation over a circular shoal due to strong refraction effect. Since then, use of the energy balance equation has become a routine work in harbor planning and structural designs in Japan.

Another important application of directional wave spectrum is the analysis of wave diffraction by breakwaters. Figure 4 is an example of comparison between the monochromatic and directional random waves concerning the heights of waves diffracted through an opening, the width of which is equivalent to five times the wavelength, after Nagai.[20] The left diagram is for monochromatic waves and the right diagram is for directional random waves. The solid curves represent the contours of the ratio of the diffracted to the incident wave heights, while the dashed curves show the wave period ratio. The difference between the monochromatic and directional random wave diffraction is so large that it has led to the disuse of monochromatic diffraction diagrams for actual harbor designs.

Following Nagai's work, Goda and Suzuki[12] prepared several sets of random wave diffraction diagrams of semi-infinite breakwaters and breakwater openings for waves having the Mitsuyasu-type directional spectrum with $s_{\max} = 10$, 25 and 75. These sets of random wave diffraction diagrams have been used as the standard design tools in Japan. When Goda *et al.*[21] presented these sets to American and European coastal engineers in 1978, they showed little interest in them, probably because of their unfamiliarity with the concept of directional wave spectrum. They began to employ directional wave spectra in their computational works only after Vincent and Briggs[22] reported their laboratory measurements on the refraction and diffraction of random waves over an elliptical shoal.

The energy balance equation of Eq. [10] is often employed for computation of the shoaling and refraction of directional random waves over a large area, but it cannot deal with wave diffraction as

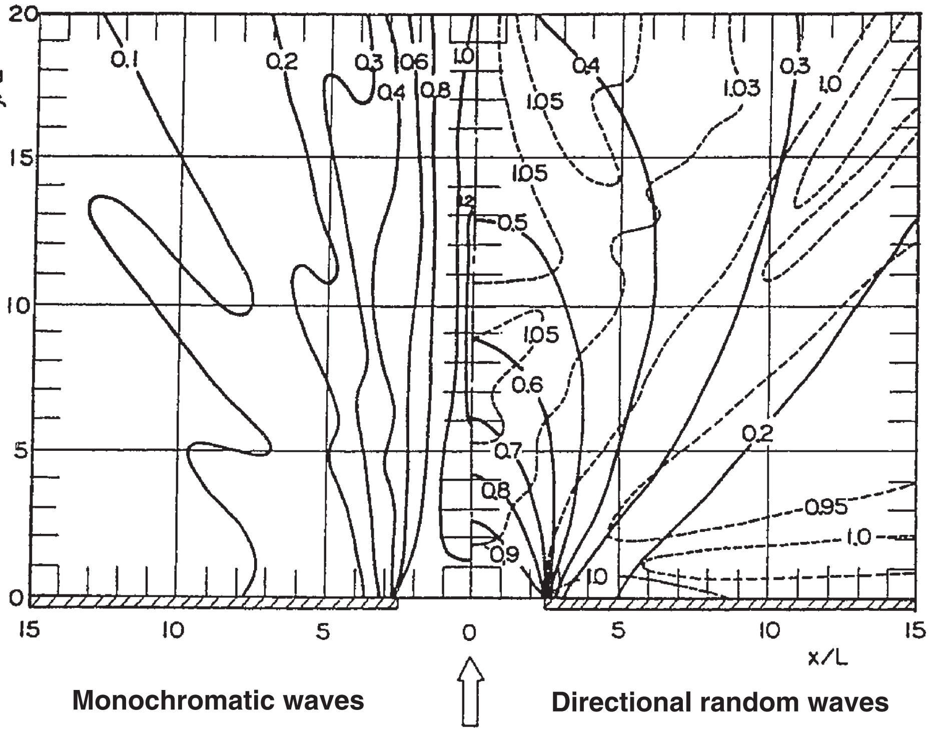

Fig. 4. Comparison of monochromatic and directional random wave diffraction diagrams through a breakwater opening of $B = 5L$ after Nagai.[20)]

well as wave attenuation by depth-limited breaking. The SWAN (Simulating WAves in the Nearshore) model by Holthuijsen *et al.*[23)] incorporates the wave breaking process by means of the bore model by Battjes and Janssen,[24)] but it requires an approximate modification to solve the wave diffraction problem.[25)] There are several models based on the parabolic equation which was initially derived by Radder[26)] from the mild slope equation and is capable of handling the wave diffraction process. Among them, the PEGBIS (Parabolic Equation with Graduational Breaker Index for Spectral waves) model by Goda[27)] can analyze the depth-limited wave breaking process quite in detail currently.

The numerical models mentioned above are the so-called phase-averaged models that can predict the spatial distribution of wave amplitude but no information on the phases of wave components. Another type of numerical model is called the time-domain evolution model that tracks down the evolution of spatial wave profiles in a given computational domain. Several numerical models based on the Boussinesq equation have been developed and utilized in engineering applications, even though the computational load is quite high with the CPU time being counted by the units of days for conventional desk computers.

Breaking of random waves

Among various nonlinear physical processes, water waves are unique in having a spectacular feature of breaking that destroys the continuity of motion. Wave breaking is not only fascinating and impressive, but it also exercises large influence on engineering applications. Many maritime structures have to be designed against the maximum load produced by breaking waves. Breaking waves on a beach hit the sea bottom and bring up a dense cloud of suspended sediment, which is carried by the nearshore currents induced by breaking waves themselves. The process causes morphological changes of beach in erosion and accretion.

Observation of the breaking of regular waves in laboratories is not difficult. Many laboratory data have been compiled in a set of relationships among the breaking wave height, water depth at breaking, offshore wave height and period, and beach slope.

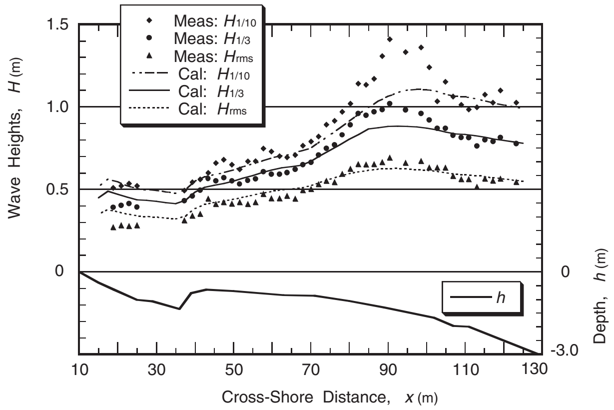

Fig. 5. Comparison of wave heights $H_{1/10}$, $H_{1/3}$ and H_{rms} at Ajigaura Beach observed by Hotta and Mizuguchi[30] and those calculated by Goda.[27]

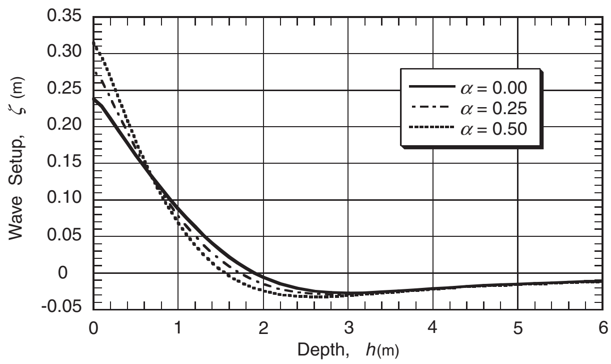

Fig. 6. Example of wave setdown and setup by random waves of $(H_{1/3})_0 = 2.0\,\mathrm{m}$, $T_p = 9.1\,\mathrm{s}$ and $\theta_0 = 30°$ on a beach with slope of 1/20 after Goda.[31]

Breaking of random waves is difficult to grasp, however, because each wave in a train of random waves breaks at a different location and each wave is attenuated differently after breaking. In 1970, Collins[28] presented a first model of wave deformation by random breaking by eliminating the portion of the probability density function of Eq. [1] that exceeds the depth-controlled breaking limit. Since then, a number of random wave breaking models have been developed and employed in various applications. Goda's model[29] in 1975 is still being used by practitioners. The bore model by Battjes and Janssen[24] is another one having been used over many years.

Figure 5 is an example of wave height variations on a beach, which were measured by Hotta and Mizuguchi.[30] They analyzed the time records of surface profiles at nearly 120 locations across the beach, which were converted from the motion-picture films taken with 12 cameras set on a nearby pier at Ajigaura Beach, Ibaraki Prefecture. The representative wave heights of $H_{1/10}$, $H_{1/3}$ and H_{rms} are shown with symbols in the upper part and the beach profile is depicted in the lower part.

Against the observed wave heights, the calculated values by means of the PEGBIS model[27] are indicated with the dash-dots, solid line, and the dotted line for $H_{1/10}$, $H_{1/3}$ and H_{rms}, respectively. In the area of $x = 80$ to $110\,\mathrm{m}$ from the shore, the observed heights, especially of $H_{1/10}$, exhibit noticeable increase over the calculated values owing to the nonlinear shoaling process. The increase is apparent one due to the change of wave profiles with sharpening of wave crests and flattening of wave troughs without changing the energy density level. Except for the area of such apparent nonlinear shoaling, the variation of wave heights across a beach is well predicted by the PEGBIS model.

Hydrodynamics of surf zone

The area where some waves are breaking is called the surf zone. In the example of Fig. 5, the area of $x = 10$ to about $100\,\mathrm{m}$ is regarded as the surf zone. Decrease of wave heights within the surf zone is related to the attenuation of wave energy density and the so-called radiation stresses, which are associated with the wave momentum flux, also vary. The spatial variation of the radiation stresses causes the change in the spatial mean water level. The lowering of the mean water level occurs at the middle of the surf zone and is called the wave setdown. The rise of the mean water level near the shoreline is called the wave setup.

Figure 6 is an example of wave setdown and setup on a uniform beach slope of 1/20 computed by the PEGBIS model.[31] The deepwater significant wave is given the height of $(H_{1/3})_0 = 2.0\,\mathrm{m}$ and the spectral peak period of $T_p = 9.1\,\mathrm{s}$ with the deepwater incident angle of $\theta_0 = 30°$ without directional spreading. The beach is assumed to have the shore-parallel, straight depth-contour with the slope of 1/20. The parameter α in the legend denotes the rate of the energy transfer from broken waves to the surface roller formed in the front face of broken waves. The rate of $\alpha = 0$ means no energy transfer, while $\alpha = 0.5$ represents a 50% transfer; the latter rate is considered as common for waves on beach.

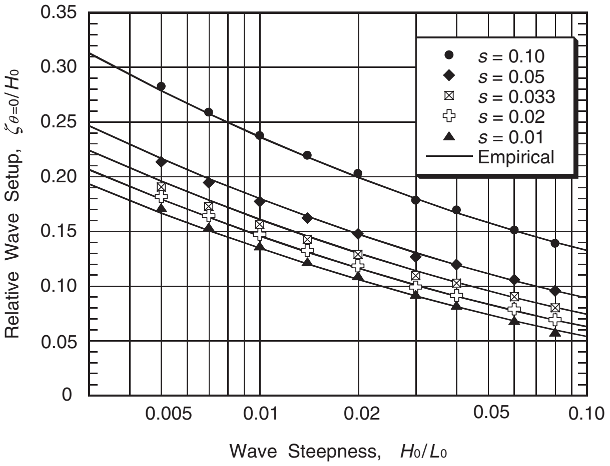

Fig. 7. Design diagram of relative wave setup $\zeta_{\theta_0=0}/H_0$ for waves of normal incidence after Goda[32] (s in the legend denotes the beach slope).

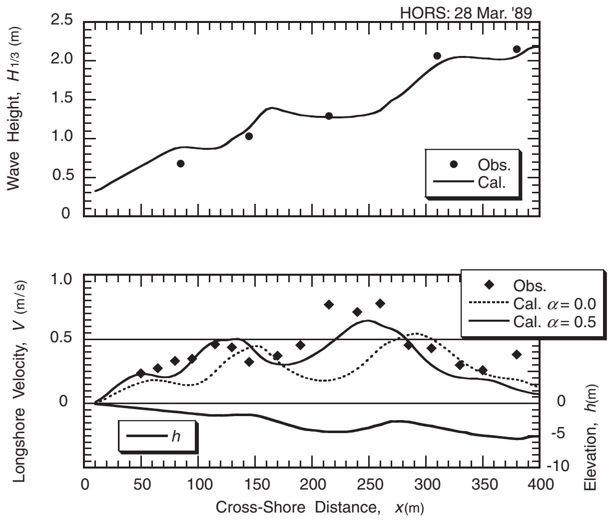

Fig. 8. Examples of significant wave height $H_{1/3}$ and longshore current velocity V across Hazaki Beach for waves of $(H_{1/3})_0 = 2.35\,\mathrm{m}$, $T_p = 9.75\,\mathrm{s}$ and $\theta_0 = 25°$: Comparison between measurements by Kuriyama and Ozaki[33] and prediction by the PEGBIS model by Goda.[31]

For the condition calculated, the wave setdown occurs in the area with the depth greater than about 2 m (40 m from the shoreline) with the maximum value of about 0.03 m. The wave setup at the shoreline is up to about 0.32 m, or 16% of the incident deepwater significant wave height.

Goda[32] has computed the amount of wave setup at the shoreline, by assuming a certain combination of spectral peak enhancement factor γ of Eq. [2] and the maximum spreading parameter $s_{\max}$ of Eq. [6] for waves with various steepness and incident angles on beaches of different slopes. Figure 7 shows a design diagram for the dimensionless wave setup at the shoreline. The symbols are the result of numerical computation and the curves represent the empirical functions fitted to the data; please refer to Goda[32] for the empirical functions and the cases of oblique incidence.

Wave-induced currents can be estimated with the information of the spatial gradients of the radiation stresses and the surface roller energy, which are evaluated through application of appropriate random wave breaking models. Figure 8 is an example of the estimation of longshore current profiles[31] being compared with the field measurements by Kuriyama and Ozaki[33] at Hazaki Beach, Ibaraki Prefecture. The upper panel shows the measured and computed significant wave heights $H_{1/3}$ across the beach for the incident deepwater wave of $(H_{1/3})_0 = 2.35\,\mathrm{m}$, $T_p = 9.75\,\mathrm{s}$ and $\theta_0 = 25°$. Waves were assumed to have the JONSWAP-type frequency spectrum with the peak enhancement factor of $\gamma = 2.0$ and the Mitsuyasu-type directional spreading function of $s_{\max} = 25$, having been selected on the basis of the wave steepness.

Hazaki Beach, the profile of which is shown at the bottom of the lower panel, had two bars at the distance of around 140 and 280 m from the baseline. The longshore currents exhibited peak velocities at the trough areas shoreward of the respective bars. Computation with the surface roller energy transfer factor of $\alpha = 0.5$ yielded the estimated velocities almost in agreement with the measured ones.

Random wave actions on maritime structures

Evaluation of the wave forces acting on breakwaters is the most important task for harbor engineers in assuring the minimum safety of breakwaters under design while keeping the construction cost under control. In case of a composite breakwater that consists of an upright section (mostly caisson, i.e., reinforced concrete box filled with sand) set on a rubble mound foundation, the structural safety is governed by the horizontal wave force acting on the front wall and the upright force under the bottom. Currently the wave forces on composite breakwaters are evaluated against the maximum wave having the height being 1.8 times the design significant wave height or the breaker height at the site, whichever the smaller one. The practice was proposed by Goda[34),35)] in 1973 together with his formulas for wave pressure calculation, and it has been adopted in maritime design manuals internationally.

In case of a mound breakwater, selection of the appropriate size of armor stones and/or concrete blocks at the surface layer to protect the core part of the breakwater is the main design consideration. The representative diameter of armor units is proportional to the design wave height in general, and a number of laboratory wave flume tests have been carried out by using random waves in many countries. Several formulas using the significant wave height as the design parameter have been developed and being used for breakwater designs.

In case of dikes and seawalls to protect the land from invasion of the sea, the amount of sea water overtopping the structures by wave actions is the primary design factors. In 1975, Goda *et al.*[36)] have compiled a set of design diagrams for estimation of the mean rate of water overflowing the crests of vertical and sloped seawalls by wave actions, based on several series of laboratory tests using random waves. The design diagrams have been used as the basic design tools in planning and designing coastal protection structures in Japan. Recently, Goda[37),38)] has proposed the following unified formulas for estimation of wave overtopping rate of vertical and sloped seawalls

$$\frac{q}{\sqrt{gH_{s,toe}^3}} = q^* = \exp\left[-\left(A + B\frac{h_c}{H_{s,toe}}\right)\right] \quad [12]$$

where q denotes the mean rate of wave overtopping of seawall, $H_{s,toe}$ is the significant wave height at the toe of seawall, h_c is the crest elevation above the design water level, and A and B are the intercept and gradient coefficients, respectively, which are estimated as follows:

$$A = A_0 \tanh[(0.956 + 4.44\tan\theta) \times (h_t/H_{s,toe} + 1.242 - 2.032\tan^{0.25}\theta)] \quad [13]$$

$$A_0 = 3.4 - 0.734\cot\alpha_s + 0.239\cot^2\alpha_s - 0.0162\cot^3\alpha_s \quad : \quad 0 \le \cot\alpha_s \le 7 \quad [14]$$

$$B = B_0 \tanh\lfloor(0.822 - 2.22\tan\theta) \times (h_t/H_{s,toe} + 0.578 + 2.22\tan\theta)\rfloor \quad [15]$$

$$B_0 = 2.3 - 0.5\cot\alpha_s + 0.15\cot^2\alpha_s - 0.011\cot^3\alpha_s \quad : \quad 0 \le \cot\alpha_s \le 7 \quad [16]$$

where θ is the angle of beach measured from the horizontal, α_s is the slope angle of the front face of seawall measured from the horizontal ($\alpha_s = 90°$ for vertical seawall), and h_t is the water depth in front of the seawall.

Equations [12] to [16] indicate that the wave overtopping rate is proportional to the 3/2 power of the significant wave height at the site of the seawall, being controlled by the crest elevation relative to the significant wave height. With lowering in the relative crest elevation $h_c/H_{s,toe}$, the wave overtopping rate increases exponentially. The wave overtopping rate is further affected by the relative toe depth $h_t/H_{s,toe}$, the beach slope $\tan\theta$ and the seawall front slope $\cot\alpha_s$.

As exemplified above, wave actions on maritime structures are evaluated with either the maximum or the significant wave height under due consideration of wave randomness.

Random waves and coastal sediment problems

Compared with the problems related to wave transformations and actions on structures, coastal sediment problems are still mostly dependent on the regular wave approach. Quite a number of researches are conducted by using the theory of regular waves or the laboratory knowledge gained through regular wave tests. Surf zone hydrodynamics are often represented with the solutions based on breaking of regular waves. Recently there appear a few papers using random wave breaking models in computations of wave-induced currents in the surf zone and sediment transport. It is expected that further research efforts will be put on this line of approach.

One of the unsolved problems in coastal sediment transport and beach morphology seems to be the reliable evaluation of sediment pickup rate for suspension by the action of randomly breaking waves. Intermittent occurrence of heavy sediment suspension by breaking waves is difficult to record quantitatively with instruments although it is easy to recognize visually. Sediment suspension, transport by nearshore currents and sedimentation onto the bottom are governed by the fall velocity of sediment, which is a function of the sediment diameter. Because the sand grain in beach morphology problems has the range of 0.1 to 1 mm approximately, small scale tests on sediment suspension fails to simulate the prototype correctly.

Several future tests in large wave flumes which are capable of generating random waves of a few meters high would provide the key information for development of much reliable prediction of future beach morphology.

Concluding remarks

Over the past sixty years, our knowledge on the random nature of sea waves has advanced greatly. Research efforts by physical oceanographers clarified the spectral characteristics of ocean waves and coastal dynamics. The knowledge gained by them was gradually digested by coastal engineers and applied for marine structure construction and coastal protection works. Nowadays the random wave concept plays the central role in coastal engineering practice. Incorporation of random wave concept in coastal morphological problems would be the task to be carried out by the next generation of coastal engineers.

The present overview covers only a part of the subjects being dealt with in coastal engineering. Field wave measurements, extreme statistics of storm waves, development of probability-based design method, and others are those on the hardware side. Ecological improvement of beach areas, enhancement of biomass in tidal flats and shallow water, improvement of water quality in embayment, and others are those on the software side. Coastal engineers in Japan and in the world are trying hard for bringing better life for all.

References

1) Sverdrup, H.U. and Munk, H.M. (1946) Empirical and theoretical relations between wind, sea, and swell. Trans. American Geophys. Union **27**, no. 6, 823–827.
2) Sverdrup, H.U. and Munk, H.M. (1947) Wind, Sea, and Swell; Theory of Relations for Forecasting. U.S. Navy Hydrographic Office, H.O. Pub. no. 601.
3) Deacon, G. E. R. (1952) Analysis of sea waves. Gravity Waves, Proc. NBS Semicentennial Symp. on Gravity Waves, National Bureau of Standards Circular **521**, 209–214.
4) Neumann, G. (1953) On ocean wave spectra and a new method of forecasting wind-generated sea. Beach Erosion Board, U.S. Army Corps of Engineers, Tech. Memo. **43**, 1–42.
5) Pierson, W. J. Jr., Neumann, G. and James R.W. (1955) Practical Methods of Observing and Forecasting Ocean Wave by Means of Wave Spectra and Statistics. U.S. Navy Hydrographic Office, H.O. Pub. no. 603.
6) Bretschneider, C.L. (1959) Wave variability and wave spectra for wind-generated gravity waves. Beach Erosion Board, U.S. Army Corps of Engineers, Tech. Memo. **118**, 1–192.
7) Mitsuyasu, H. (1970) On the growth of spectrum of wind-generated waves (2) — spectral shape of wind waves at finite fetch. Proc. 17th Japanese Conf. Coastal Eng., 1–7 (in Japanese).
8) Pierson, W. J. Jr. and Moskowitz, L. (1964) A proposed spectral form for fully developed wind sea based on the similarity theory of S. A. Kitaigorodoskii. J. Geophys. Res. **69**, no. 24, 5181–5190.
9) Hasselmann, K., Barnett, T. P., Bouws, E., Carlson, D.E. and Hasselmann, P. (1973) Measurements of wind-wave growth and swell decay during the Joint North Sea Wave Project (JONSWAP). Deutche Hydr. Zeit, Reihe A **8**, no. 12, 1–95.
10) Goda, Y. (1988) Statistical variability of sea state parameters as a function of a wave spectrum. Coastal Eng. in Jpn., JSCE **31**, no. 1, 39–52.
11) Mitsuyasu, H., Tasai, F., Suhara, T., Mizuno, S., Ohkusu, M., Honda, T. and Rikiishi, K. (1975) Observation of the directional spectrum of ocean waves using a cloverleaf buoy. J. Phys. Oceanogr. **5**, 750–760.
12) Goda, Y. and Suzuki, Y. (1975) Computation of refraction and diffraction of sea waves with Mitsuyasu's directional spectrum. Tech. Note of Port and Harbour Res. Inst. **230**, 1–45 (in Japanese).
13) Ewans, K. C. (2001) Directional spreading in ocean swell. Proc. Int. Symp. WAVES 2001, San Francisco, ASCE, 517–529.
14) Longuet-Higgins, M. S. (1952) On the statistical distribution of the heights of sea waves. J. Marine Res. **IX**, no. 3, 245–266.
15) Goda, Y. and Kudaka, M. (2007) On the role of spectral width and shape parameters in control of individual wave height distribution. Coastal Eng. J. **49**, no. 3, 311–335.
16) Goda, Y. (2000) Random Seas and Design of Maritime Structures (2nd ed.), World Scientific, Singapore, 1–443.
17) Pierson, W. J. Jr., Tuttell, J. J. and Woolley, J. A. (1952) The theory of the refraction of a short crested Gaussian sea surface with applications to the northern New Jersey Coast. Proc. 3rd Conf. Coastal Eng., 685–692.
18) Karlsson, T. (1969) Refraction of continuous ocean wave spectra. Proc. Amer. Soc. Civil Engrs. **95** (WW4), 471–490.
19) Nagai, K., Horiguchi, T. and Takai, T. (1974) Computation of directional spectral deepwater waves propagating into shallow water area. Proc. 21st Japanese Conf. Coastal Eng., 437–448 (in Japanese).
20) Nagai, K. (1972) Computation of refraction and diffraction of irregular sea — refraction of irregular deepwater wave on slopes with parallel,

straight depth contours, and diffraction diagrams of irregular waves for breakwaters by means of linear superposition method —. Rept. Port and Harbour Res. Inst. **11**, no. 2, 47–119 (in Japanese).
21) Goda, Y., Takayama, T. and Suzuki, Y. (1978) Diffraction diagrams for directional random waves. Proc. 16th Int. Conf. Coastal Eng., Hamburg, ASCE, 628–650.
22) Vincent, C. L. and Briggs, M. J. (1989) Refraction-diffraction of irregular waves over a mound. J. Waterways, Port, Coastal and Ocean Eng. **115**, no. 2, 269–284.
23) Holthuijsen, L.H., Booji, N. and Ris, R.C. (1993) A spectral wave model for the coastal zone. Proc. 2nd Int. Symp. on Ocean Wave Measurement and Analysis, New Orleans, ASCE, 630–641.
24) Battjes, J.A. and Janssen, J.P.F.M. (1978) Energy loss and set-up due to breaking of random waves. Proc. 16th Int. Conf. Coastal Eng., Hamburg, ASCE, 1–19.
25) Booji, N., Holthuijsen, L.H., Doorn, N. and Kieftenburg, A.T.M.M. (1997) Diffraction in a spectral wave model. Proc. 3rd Int. Symp. on Ocean Wave Measurement and Analysis, Virginia Beach, Virginia, ASCE, 243–255.
26) Radder, A.C. (1979) On the parabolic equation method for wave-wave propagation. J. Fluid Mech. **95**, 159–176.
27) Goda, Y. (2004) A 2-D random wave transformation model with gradational breaker index. Coastal Eng. J. **46**, no. 1, 1–38.
28) Collins, I.I. (1970) Probabilities of breaking wave characteristics. Proc. 12th Int. Conf. on Coastal Eng., Washington, D.C., ASCE, 399–414.
29) Goda, Y. (1975) Irregular wave deformation in the surf zone. Coastal Eng. in Jpn., JSCE **18**, 13–26.
30) Hotta, S. and Mizuguchi, M. (1980) A field study of waves in the surf zone. Coastal Eng. in Jpn., JSCE **23**, 59–79.
31) Goda, Y. (2006) Examination of the influence of several factors on longshore current computation with random waves. Coastal Eng. **53**, no. 2–3, 157–170.
32) Goda, Y. (2008) Wave setup and longshore currents induced by directional spectral waves: Prediction formulas based on numerical computation results. Coastal Eng. J. **50**, no. 4 (in press).
33) Kuriyama, Y. and Ozaki, Y. (1996) Wave height and fraction of breaking waves on a bar-trough beach — field measurements at HORS and modeling —. Rept. Port and Harbour Res. Inst. **35**, no. 1, 1–38.
34) Goda, Y. (1973) A new method of wave pressure calculation for the design of composite breakwaters. Rept. Port and Harbour Res. Inst. **12**, no. 3, 31–69 (in Japanese).
35) Goda, Y. (1974) New wave pressure formulae for composite breakwater. Proc. 14th Int. Conf. on Coastal Eng., Copenhagen, ASCE, 1702–1720.
36) Goda, Y., Kishira, Y. and Kamiyama, Y. (1975) Laboratory investigation on the overtopping rate of seawalls by irregular waves. Rept. Port and Harbour Res. Inst. **14**, no. 4, 3–44 (in Japanese).
37) Goda, Y. (2008) Proposal of unified formulas for wave overtopping rate of seawalls based on CLASH database. Annual J. Civil Eng. in the Ocean, JSCE **24**, 939–944 (in Japanese).
38) Goda, Y. (2008) Derivation of unified wave overtopping formulas for seawalls with smooth, impermeable surfaces based on selected CLASH datasets. Coastal Eng. **55** (in press).

(Received July 24, 2008; accepted Aug. 18, 2008)

Profile

Yoshimi Goda was born in 1935 and pursued his career of research engineer for 31 years at the Port and Harbour Research Institute, Ministry of Transport, since his graduation from the University of Tokyo in 1957. While he served there, he attended the Graduate School of Massachusetts Institute of Technology from 1961 to 1963 and graduated with the M.Sc. degree. He was awarded the Doctorate degree in Engineering from the University of Tokyo in 1976. His research works from 1957 to 1988 covered the problems of design wave force on vertical breakwaters, harbor resonance, random sea waves and their actions on structures, extreme statistics of storm waves, and others. He served as the Director General of the Port and Harbour Research Institute for two years before he joined the Faculty of Engineering of Yokohama National University in April, 1988. Upon his retirement in March 2000 he was given the title of Professor Emeritus at Yokoyama National University.

He is a pioneer in the field of engineering applications of random sea waves as exemplified by his book "Random Seas and Design of Maritime Structures" from the University of Tokyo Press in 1985. He published its second edition from World Scientific in 2000, and currently working for the third edition to be published in 2009. For his distinguished research accomplishments, he has received the International Coastal Engineering Award of the American Society of Civil Engineers in 1989, the Outstanding Achievement Award (2003), the Paper Prize (1976), and the Incentive Paper Prize (1967) of the Japan Society of Civil Engineers, and the Award for Eminent Research Accomplishments (1976) and the Transport Culture Award (1999), both by the Minister of Transport. He is the Honorary Member of the Japan Society of Civil Engineering. In November 2006, the Emperor of Japan awarded him the Middle Order of Sacred Treasure with blue ribbon.